

# Investigation of horizontal performance of levee consisting of double sheet pile walls and partition walls by 1-g model tests

K. Toda

Chief, Construction Solutions Development Department, Giken LTD., Kochi, Japan

Y. Ishihara

Manager, Construction Solutions Development Department, Giken LTD., Kochi, Japan

A. Canning

Department of Engineering, University of Cambridge, Cambridge, UK

S. K. Haigh

Professor of Geotechnical Engineering, Department of Engineering, University of Cambridge, Cambridge, UK

## ABSTRACT

In Japan, the tsunami damage and liquefaction caused by the Great East Japan Earthquake of 2011 and the torrential rains caused by typhoons in recent years have created a need for levees with a tenacious structure. As one of the countermeasures, levees fitted with double sheet pile walls at their shoulders have been proposed. Furthermore, levees with partition walls that divide the ground sandwiched by the double sheet pile walls have also been proposed. Although it has been confirmed that the levees with double sheet pile walls and partition walls are more effective in restricting their deformation due to liquefaction, they have not been tested against horizontal loads caused by flood or tsunami. In this study, a 1-g model experiment was conducted to confirm the effect and working of the partition walls against horizontal loads. The sheet pile walls and the partition walls were modeled using acrylic plates. The acrylic plates were divided into pieces, with each piece representing a sheet pile. The results showed that horizontal loads were transferred from the front side to the rear side of the double sheet pile walls via the partition walls and that the horizontal resistance was improved.

**Key words:** Levee, Double sheet pile walls, Partition walls, 1-g model experiment, Horizontal resistance

## 1. Introduction

In Japan, the tsunami damage and liquefaction caused by the Great East Japan Earthquake of 2011 and the torrential rains caused by typhoons in recent years have created a need for levees with a tenacious structure. As one of the countermeasures, levees fitted with double sheet pile walls at their crest have been proposed. The effectiveness of these structures to safeguard against earthquakes and overflow was confirmed through model tests (Otsushi et al., 2010). The behavior of these structures under tsunami loads was confirmed through Finite Element Method (FEM) analysis (Furuichi et al., 2015). Furthermore, levees with partition walls that divide

the ground sandwiched by the double sheet pile walls were also proposed as shown in Fig. 1.

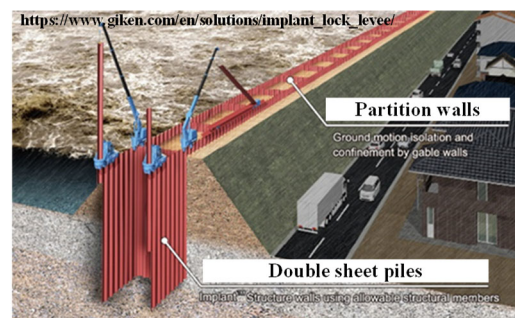


**Fig. 1** Application of levees with partition walls

Although it has been confirmed that levees with double sheet pile walls and partition walls are more

effective in restricting the deformation of structures due to liquefaction (Fujiwara et al., 2018), they have not been tested against horizontal loads caused by flood or tsunami.

In this study, since the partition walls are expected to increase the horizontal resistance of the structure, a 1-g model experiment was conducted to confirm the effect and working of the partition walls. The sheet pile walls and the partition walls were modeled using acrylic plates in some test cases. The acrylic plates were divided into pieces, with each piece representing a sheet pile that behaves individually.

**2. Methods of model tests**

**2.1. Test cases**

As shown in Fig. 2, four cases with and without the partition walls were used in the model test. In all the cases, acrylic plates 600 mm long, 400 mm wide and 5 mm thick were used as the double sheet pile walls. In order to take into account the relative sliding between each sheet pile in the partition walls and the actual condition where the top of the levee will be covered with concrete panels, the partition walls were “unconstrained” in Case No. 2, the double sheet pile walls and the partition walls were “constrained” on top of each other in Case No. 3, and these models were “fully constrained” in Case No. 4.

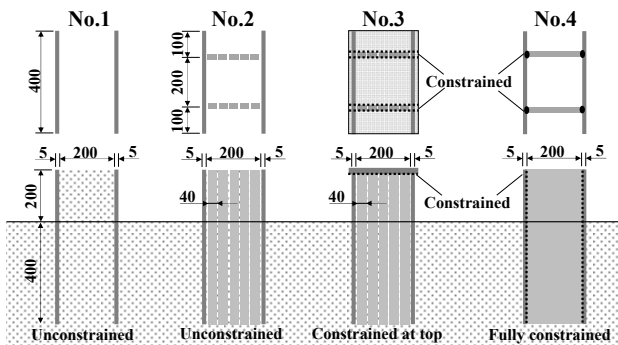


Fig. 2 Test cases

The double sheet pile walls and the partition walls were modeled using acrylic plates as shown in Table 1. Considering the similarity law regarding bending stiffness, acrylic plates of 5 mm thickness were chosen. As shown in Table 2, this corresponds to the sheet pile SP-IVw (of 600 mm width), which was used in the construction of the Implant™ levee on the Nino coast (Ishihara et al., 2020). In Case No. 2, the acrylic plates for the partition walls were divided into five pieces of width 40 mm each. In

Case No. 3, the same acrylic plates as in Case No. 2 were used, but the relative vertical displacements and rotations were constrained at top of the double sheet pile walls and the partition walls. In Case No. 4, the partition walls were modeled using a plate of width 200 mm without any division.

Table 1 Characteristic values of acrylic plates

Specific gravity	g/cm <sup>2</sup>	1.19
Tensile strength	N/mm <sup>2</sup>	73
Flexural strength	N/mm <sup>2</sup>	113
Flexural modulus	N/mm <sup>2</sup>	3200

Table 2 Model similarity rule of double sheet pile walls

			SP-IVw	Acrylic plate
Width of sheet pile	$W_s$	[mm]	600	20
Sectional secondary moment	$I$	[cm <sup>4</sup> ]	8,630	0.021
Young's modulus	$E$	[N/mm <sup>2</sup> ]	205,000	3,200
Bending stiffness	$EI$	[Nmm <sup>2</sup> ]	17,692x10 <sup>9</sup>	0.667x10 <sup>6</sup>

**2.2. Apparatus**

A soil tank of 800 mm height, 1030 mm width, and 400 mm depth was used, as shown in Fig. 3. The model ground was made of silica sand #6, as shown in Fig. 4.

In the preparation of the ground and setting up of the model, the first step was to fill, level, and tamp down the soil so that the layer thickness was about 50 mm and set up of the model above the layer thickness was 200 mm, as shown in Fig. 5 (1) and (2). Next, similar to the first step, sand was filled in the same order on the right side, left side, and center of the model, as shown in Fig. 5 (3). Finally, once the layer thickness reached 600 mm, sand was placed in the center of the model, as shown in Fig. 5 (4). Here, the edges of the double sheet pile walls were in contact with only the soil tank, and displacement in the width direction (i.e. perpendicular to the loading direction) was constrained. The partition walls were not constrained during the ground preparation except the conditions determined in each test case. In all the cases, the weight of the sand was measured using four load cells installed under the soil tank corner. The relative density of the soil was calculated by considering the measured weight of the sand, as shown in Table 3. There was some variation in the relative density, with an error of about ±5%, when compared to 52.1% of the average value.

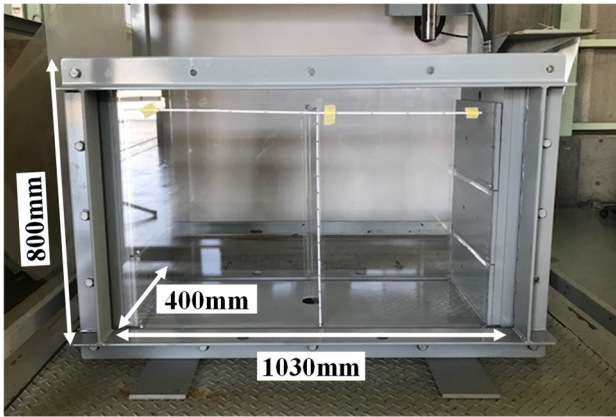


Fig. 3 Soil tank of the 1-g model experiment

Soil particle density ( g/cm <sup>3</sup> )	2.62
Maximum dry density ( g/cm <sup>3</sup> )	1.52
Minimum dry density ( g/cm <sup>3</sup> )	1.24
Internal friction angle for $D_r=60\%$ (degrees)	38.7

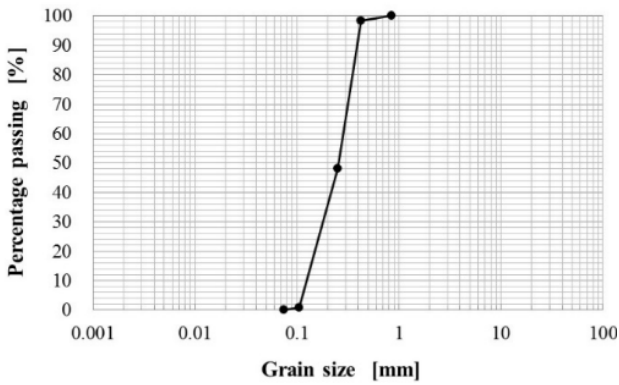


Fig. 4 Property and grain size accumulation curve of silica sand #6 (after Ishihara et al. (2015))

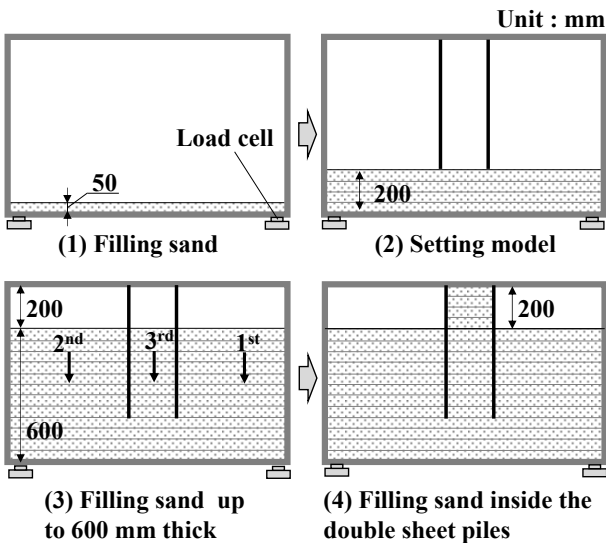


Fig. 5 Preparation of the ground and set up of the model

Table 3 Relative density of the soil in all cases

No	Volume of sand $V$ [m <sup>3</sup> ]	Weight of sand $M_s$ [kN]	Volume of sand $V_s=M_s/\rho_s$ [m <sup>3</sup> ]	Volume of void $V_v=V-V_s$ [m <sup>3</sup> ]	Void ratio $e=V_v/V_s$	Relative density $D_r$ [%]
1	0.261	3.52	0.137	0.124	0.901	53.7
2	0.260	3.53	0.137	0.122	0.891	56.3
3	0.260	3.46	0.135	0.125	0.927	47.0
4	0.260	3.49	0.136	0.124	0.909	51.6

Soil particle density:  $\rho_s = 25.7$  [kN/m<sup>3</sup>]

Maximum void ratio:  $e_{max} = 1.11$

Minimum void ratio:  $e_{min} = 0.72$

Relative density:  $D_r = (e_{max} - e)/(e_{max} - e_{min})$

### 2.3. Method of loading and measurement

The layout of the model test is shown in Fig. 6. A turnbuckle-type steel bundle was used for loading. A wooden spacer was placed between the turnbuckle-type steel bundle and the double sheet pile walls in order to allow the horizontal load to act in the width direction of the double sheet pile walls. The wooden spacer was in contact with the double sheet pile wall, so the actual deflection in the width direction due to water or earth pressure was not taken into account in Case No. 2, Case No. 3, and Case No. 4, as shown in Fig. 7. This is because it was difficult to accurately measure the loads on water or earth pressure. Displacement sensors were installed at eight locations, as shown in Fig. 8. As shown in Fig. 9, strain gauges were affixed to both sides of the double sheet pile walls to confirm the bending moment and axial stress. Triaxial strain gauges were affixed to the partition walls to check the stress distribution in the partition walls.

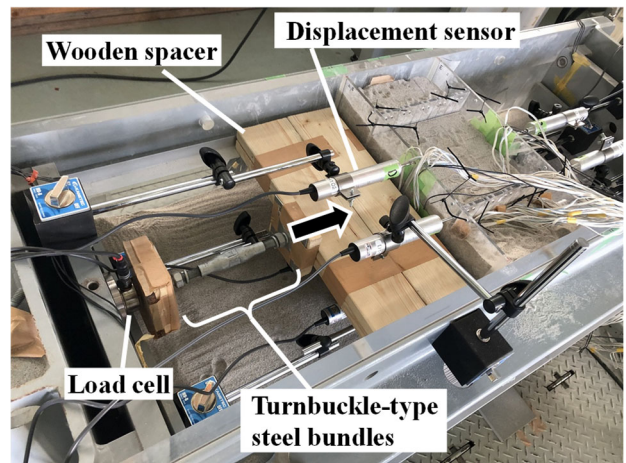


Fig. 6 Test layout

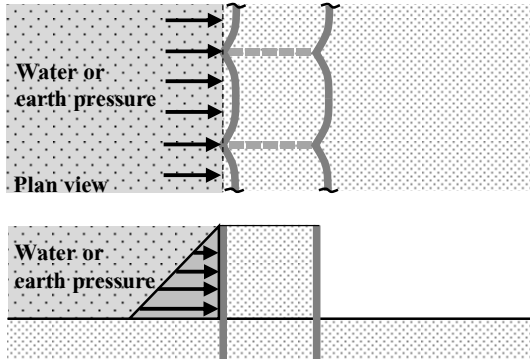


Fig. 7 Actual deflection in the width direction

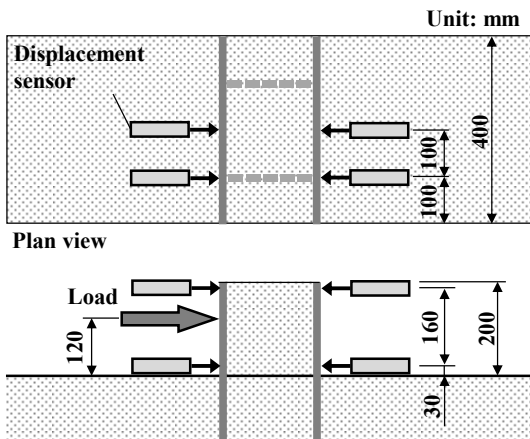


Fig. 8 Layout of the displacement sensors

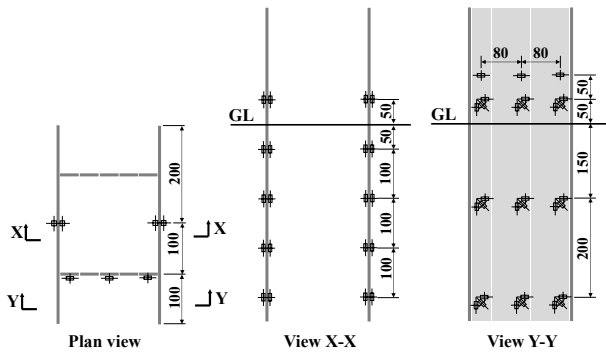


Fig. 9 Layout of strain gauges

In Case No. 1 and Case No. 2, the distance between the two sheet pile walls was maintained using cable ties, as shown in Fig. 10, to prevent them from opening up owing to the dead weight of the sand inside the levee. To eliminate the effects of cable restraint during loading, the cable ties were cut before loading in Case No. 1. In Case No. 2, the cable ties were cut when displacement at GL+0.19 m was 2 mm, which is 1% of the height of the levee, to avoid the tension introduced on the cable ties, as shown in Fig. 10.

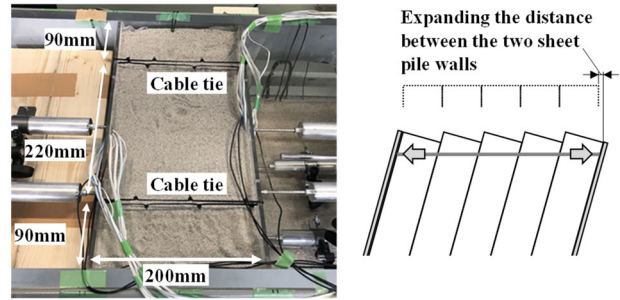


Fig. 10 Cable ties in “unconstrained” case and tension introduced on the cable ties

### 3. Results of model test

#### 3.1. Horizontal resistance

The load-displacement curves observed during the experiment are shown in Fig. 11. The displacement shown in Fig. 11 is the average value of two displacement sensors at GL+0.19m. The load shown in Fig. 11 is the value of the load cell acting on the 400 mm width. “Front” is the loading side and “Back” is the opposite side. In Case No. 2, Case No. 3, and Case No. 4, the state of the partition walls when the displacement sensor at GL+0.19m was 20 mm, as shown in Fig. 12.

In Case No. 1, when the cable was cut before loading, displacement sensors at GL+0.19 m were -3.3 mm at the “Front” and 3.2 mm at the “Back”, i.e., the total opening of the sheet pile walls was around 6.5 mm. In Fig. 11 (Case No. 1), the displacement at the start of loading was corrected to zero. The displacement at GL+0.19 m of the “Front” was greater than that of the “Back”. It is considered that the load was not transmitted sufficiently to the “Back” side.

In Case No. 2, the cable ties were cut when the displacement at GL+0.19m was 2 mm. Though the displacement of the “Back” increased rapidly, the load-displacement curve was similar to that of the “Front” during loading, as shown in Fig. 11 (Case No. 2). As shown in Fig. 12, it was confirmed that the partition walls of Case No. 2 behaved individually when compared to those of Case No. 3 and Case No. 4.

A comparison of all the cases is shown in Fig. 11. Case No. 4 had the highest resistance. Case No. 3 was equivalent to Case No. 2 despite the upper part being fixed. However, these cases had a higher resistance than Case No. 1.

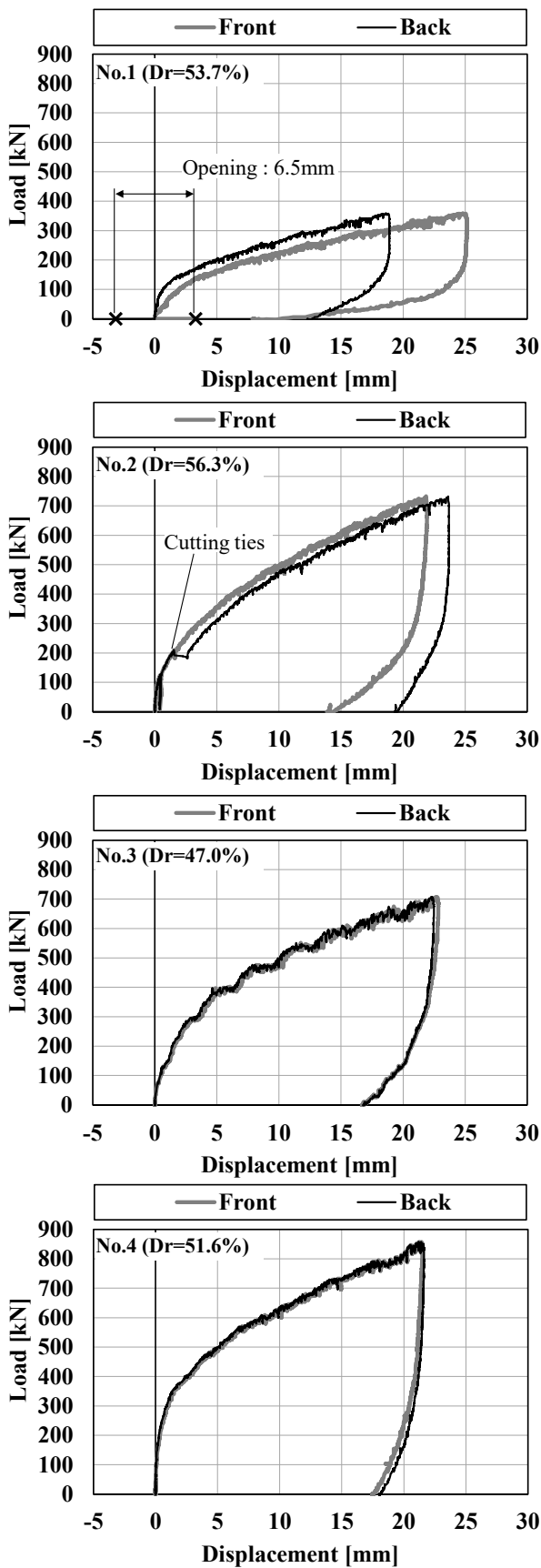


Fig. 11 Load-displacement curves obtained from the test

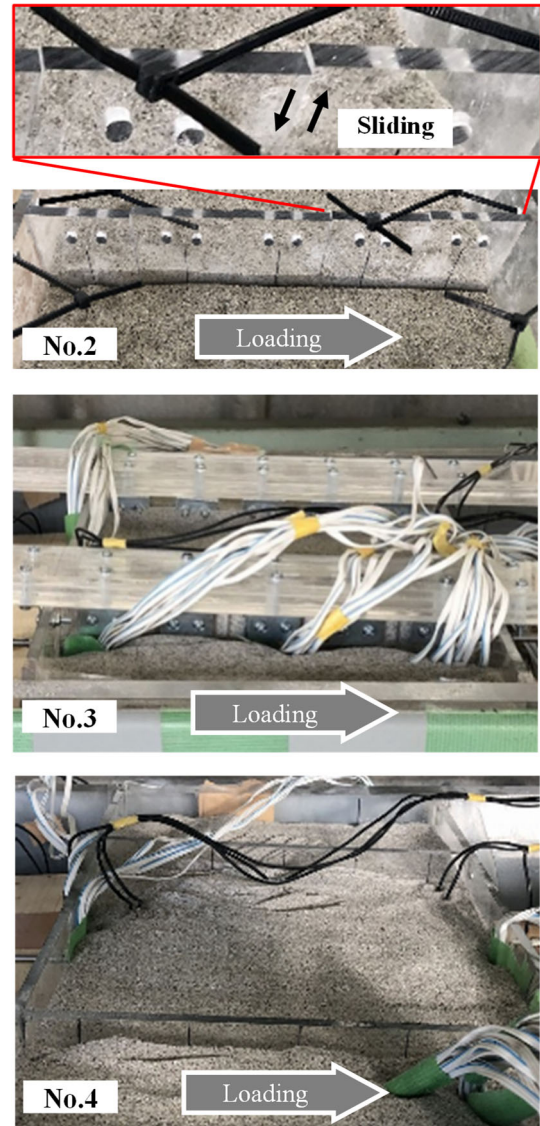


Fig. 12 State of the partition walls at a displacement of 20mm

### 3.2. Stress state of the double sheet pile walls and the partition walls

Fig. 13 shows the bending stress distribution of the double sheet pile walls for a displacement of 20 mm at GL+0.19 m. In Case No. 4, the strain gauge at GL-0.32 m was excluded because of unstable value.

In Case No. 1, the bending stress was higher than the other cases at the top side; furthermore, the bending stress of the “Front” was higher than that of the “Back”. In Case No. 2 and Case No. 3, the distribution was close to a uniformly distributed load with pin roller support. The “Front” and “Back” of these cases were approximately equal.

For the displacement of 20 mm at GL+0.19 m, the axial stress distribution of the strain gauge affixed to the

double sheet pile walls are shown in Fig. 14. The vertical stress distribution on the partition walls at GL-0.15 m is shown in Fig. 15.

In Case No. 4, the “Front” of the sheet pile was subjected to tensile stress while the “Back” was subjected to compressive stress. The vertical stress on the partition walls also changed linearly from tension to compression from “Front” to “Back”. On the other hand, the above bending stress distribution was not obtained in Case No. 3 even though the upper part was constrained.

For the displacement of 20 mm at GL+0.19 m, the maximum and minimum principal stresses in the partition walls at GL-0.15 m are shown in Fig. 16. In Case No. 2 and Case No. 3, the minimum principal stresses showed an overall downward right direction. The horizontal loads were considered to be transmitted horizontally from “Front” to “Back”. Case No. 4 displayed a different behavior when compared to Case No. 2 and Case No. 3. It showed tensile stresses in the “Front side 80 mm” and compressive stresses in the “Back side 80 mm”, which is consistent with the trend described in Fig. 15.

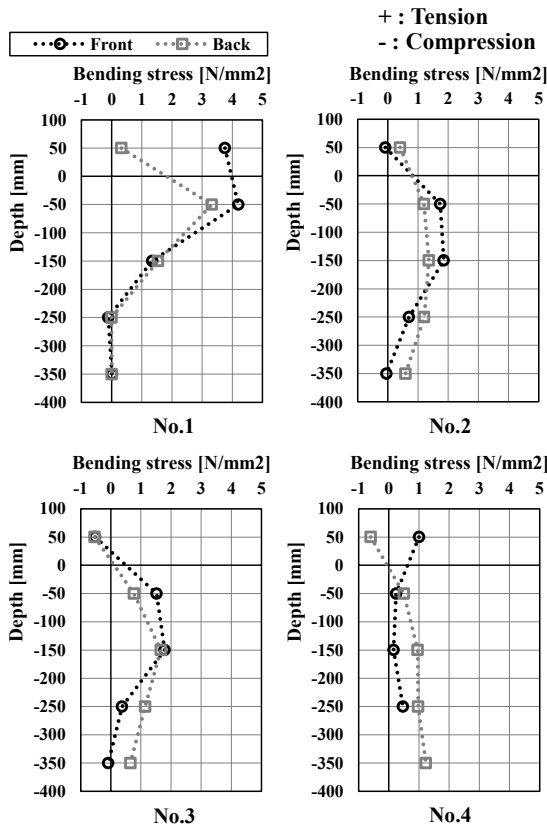


Fig. 13 Bending stress at the center of the double sheet pile walls (displacement of 20 mm at GL+0.19 m)

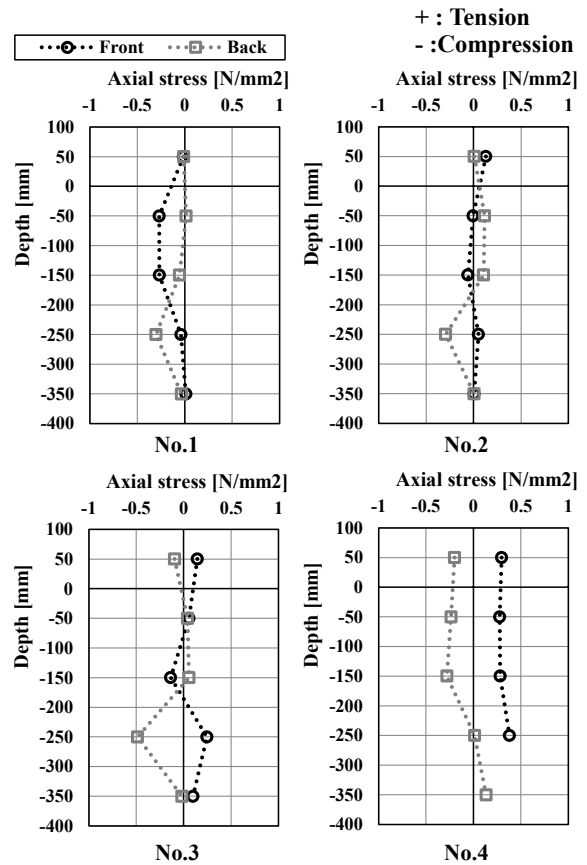


Fig. 14 Axial stress in the double sheet pile walls (when the displacement at GL+0.19m was 20 mm)

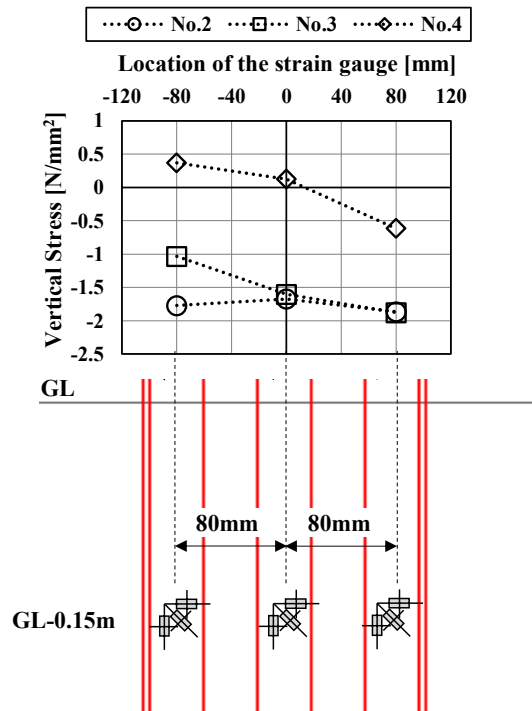


Fig. 15 Vertical stress in the partition walls at GL-0.15m (when the displacement at GL+0.19 m was 20 mm)

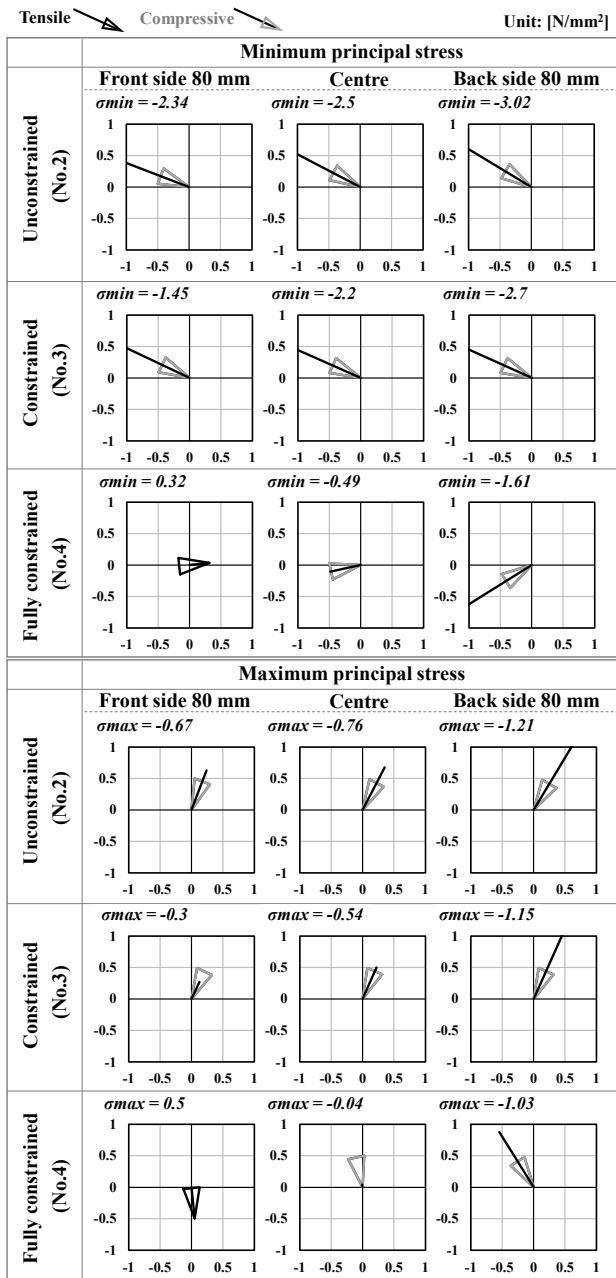


Fig. 16 Minimum and maximum principal stresses in partition walls (when the displacement at GL+0.19m was 20 mm)

### 3.3. Effect of partition walls

The effects of the partition walls were organized considering the test results shown in Fig. 17.

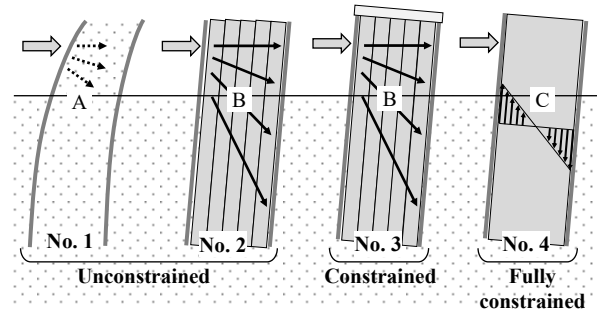
In Case No. 1, where no partition walls were installed (and hence unconstrained), it is considered that the soil in the double sheet pile wall was deformed by the compression of the soil near the loading point, and the load was not fully transferred from the “Front” to the “Back” and from the top to the bottom side.

In Case No. 2, where the partition walls were

unconstrained, it is considered that the horizontal loads were distributed over the entire double sheet pile walls via the partition walls, resulting in smaller horizontal displacements than in Case No. 1.

In Case No. 3, where the partition walls were constrained, it is considered that only the horizontal loads were transferred from “Front” to “Back” as in Case No. 2, as the partition walls were divided. Regarding the difference in behavior between Case No. 2 and Case No. 3, it was expected that the ground resistances at the partition wall base in Case No. 3 would be higher than that in Case No. 2, since the partition wall of Case No. 3 was expected to behave as a single unit, as shown in Fig. 18. However, the estimated resistance of the test results was almost the same. One reason for this may be that the relative density of Case No. 3 was lesser than that of Case No. 2.

In Case No. 4, where the partition walls were fully constrained, it is considered that not only the horizontal loads but also the shear forces were transferred from the “Front” side to the “Back” side, and a composite of the double sheet pile walls and the partition walls have undergone bending deformation.



A) Horizontal forces were transmitted through the ground and introduced to the “Front”.  
 B) Horizontal loads were transmitted through the partition walls.  
 C) Horizontal loads and shear forces were transmitted through the partition walls as bending resistance of partition walls.

Fig. 17 Comparison of horizontal resistance

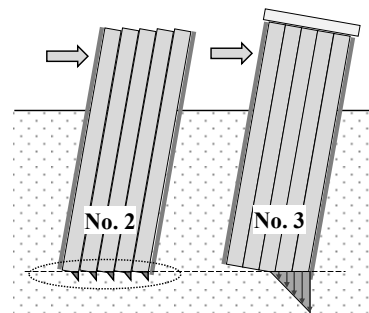


Fig. 18 Expected ground resistances at partition wall base

#### **4. Conclusions**

A 1-g model experiment was conducted to confirm the effect and working of double sheet pile walls with partition walls against horizontal loads. In addition to a case without any partition walls, model tests were conducted for three cases, differentiated by the condition of the partition walls: “unconstrained”, “constrained at the top”, and “fully constrained”, in order to take into account the relative sliding between each sheet pile in the partition walls and the actual condition that the top of the levee will be covered with concrete panels.

The results showed that the horizontal resistance was improved in all the cases with partition walls. In the “unconstrained” cases, horizontal loads were transferred from the front side to the rear side of the double sheet pile walls via the partition walls. In the “constrained” case, the horizontal resistance was equivalent to that of the “unconstrained” cases. The partition walls are considered to have been divided and only horizontal loads were transmitted. In the “fully constrained” case, horizontal resistance was the highest among all cases. It was considered that the horizontal loads and the shear forces were transmitted through the partition walls and the partition walls put forth the bending resistance.

#### **References**

- Fujiwara, K., Taenaka, S., Takahama, K., and Yashima, A. 2018. 3-D Behavior of coastal dyke installed by double sheet-piles with partition wall. *Proceedings of the First International Conference on Press-in Engineering 2018, Kochi*, pp. 257-264.
- Furuichi, H., Hara, T., Tani, M., Nishi, T., Otsushi, K. and Toda, K. 2015. Study on reinforcement method of dykes by steel sheet-pile against earthquake and tsunami disasters. *Japanese Geotechnical Journal*, Vol. 10, No.4, pp. 583-594. (In Japanese)
- Ishihara, Y., Ogawa, N., Okada, K. and Kitamura, A. 2015. Implant preload wall: a novel self-retaining wall with high performance against backside surcharge. *Proceedings of the 5th IPA International Workshop in Ho Chi Minh, Press-in Engineering 2015*, pp. 68-82.
- Ishihara, Y., Yasuoka, H. and Shintaku, S. 2020. Application of press-in method to coastal levees in Kochi Coast as liquefaction countermeasures. *Press-in Piling Case History*, Vol. 1, pp. 141-148.
- Otsushi, K., Koseki, J., Kaneko, M., Tanaka, H. and Nagao, N. 2010. Experimental study on reinforcement method of levees by sheet-pile. *Japanese Geotechnical Journal*, Vol. 6, No.1, pp.1-14. (In Japanese)